An Improved Design of the Linear Diffraction Grating Interferometer

Cheng Fang[1,#], **Fan   Kuang-Chao**[1, 2] **and Fei   Yetai**[1]

1 School of Instrument Science and Optoelectronics Engineering, Hefei University of Technology，No.193 Tunxi Road, Hefei, Anhui, 230009, China
2   Department of Mechanical Engineering, National Taiwan University，Taipei,10627,Taiwan
Corresponding Author / E-mail: chf19chf19@163.com, TEL: +86-551-2903823, FAX: +86-551-2903823

Abstract: In this study an improved design of Linear Diffraction Grating Interferometer (LDGI) is proposed. The principle of this nanometer interferometer can be attributed to phase information encoded by the ±1 diffraction light beams. Properly interfering these two beams leads to modulation similar to Doppler frequency shift which can be translated to displacement measurement via phase decoding. Compared to the earlier designs, the proposed structure has some significant improvements: 1. The optical system forms the simplest structure. 2. The high-order disturbance is weakened because this structure reduces the redundant beams. 3. The left beam and right beam are in symmetry which will eliminate the optical path difference completely. Experiments show that the proposed structure has notably improved the signal quality. With software-based signal correction and subdivision, the resolution can reach to 1nm. Calibrated by a commercial laser interferometer, this new sensor achieves the repeatability of 10nm in 15mm travelling length.

NOMENCLATURE

d: grating pitch
v: moving speed
f_0: laser beam frequency
σ : waveform distortion intensity
Δf: Doppler frequency drift

1. Introduction

Optical instruments are wildly used in length measurement [1]. Solving the paradox between the measurement range and accuracy is a challenging work. Laser interferometer is one of the most important non-contact metrology instruments for its high resolution and long measurement range, but it's expensive and sensitive to environmental conditions [2]. Conventional linear encoders have stable readings but the resolution is limited by the big pitch [1, 3].

To solve this problem, an innovative grating sensor, the Linear Diffraction Grating Interferometer (LDGI), based on Doppler phase shift, has been developed by the authors [4]. It shows good stability and accuracy but the optical system is very comprehensive [5-8]. Some earlier designs of LDGI have four fundamental disadvantages that will affect the signal quality: 1. Too many lenses will weaken the laser intensity and decrease the signal-to-noise ratio [7]; 2. Complicated reflection will cause unpredictable disturbance [7, 8]; 3. Compensation lenses with nonstandard dimension are introduced to adjust the optical path difference [8]. 4. The residual gap between two contact optics will cause unpredictable reflection [7]. Some software-based algorithms have been developed to correct the waveforms [9-

11], but the computing time is accordingly increased. In the worst case the algorithm can hardly distinguish higher-order harmonic terms. Therefore, it's necessary to simplify the optical structure and improve the signal quality.
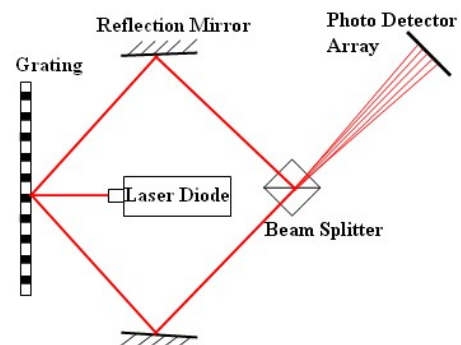
2. The Principle of LDGI

Fig. 1 Principle of grating-based interferometer

Fig. 1 shows the principle of a grating-based interferometer. the ±1 diffraction beams, with the diffraction angle determined by the laser frequency and grating pitch, will have a Doppler frequency drift expressed as [4]:

$$f_{+1} = f_0 + \frac{v}{d} \tag{1}$$

$$f_{-1} = f_0 - \frac{v}{d} \tag{2}$$

Thus, the interference fringe on the photodetector has the frequency as:

$$\Delta f = f_{+1} - f_{-1} = \frac{2v}{d} \qquad (3)$$

The fundamental principle of grating-based interferometer is to interfere the ±1 diffraction beams. With this principle an early LDGI design, with exact phase shift, has been developed, as shown in Fig. 2 [8].
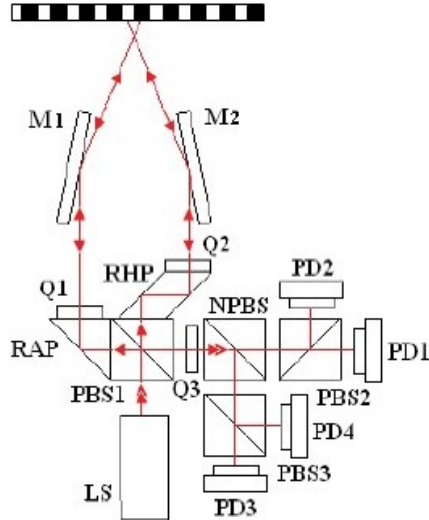

Fig. 2 A former design of LDGI (LS: laser diode, G: grating, PBSi: ith polarizing beam splitter, RAP: right angle prism, RHP: rhomboid prism, Mi: ith mirror, NPBS: non-polarizing beam splitter, Qi: ith quarter waveplate, PDi: ith photodetector.)

The laser beam is split by the polarization beam splitter (PBS1), with equal intensity. Taking the right-arm beam for instance, the P-polarized beam passes through PBS1 and is converted into a right-circular polarized beam by the quarter waveplate Q1. With the emitted angle equal to the diffraction angle, the +1 diffraction beam will go back along the same path. It is then converted into S-polarized beam after passing through Q1 again and transmits to Q3 at PBS1. It is to avoid the beam returning back to the laser diode. The left-arm beam has the similar feature. After passing through Q3 the left-arm beam and right-arm beam will be converted into right-circular and left-circular polarized beams, respectively. The NPBS divides both beams into two split beams of equal intensity. These four beams will be separated by 0-90-180-270 degrees by PBS2 and PBS3 (set fast axis to 45 degrees) and interfere with each other. Analyzed by the Jones vector, the intensity of each photodetector can be expressed as:

$$I_{PD1} = A[1 - \sin(2\Delta\omega \cdot t)] \qquad (4)$$

$$I_{PD2} = A[1 + \sin(2\Delta\omega \cdot t)] \qquad (5)$$

$$I_{PD3} = A[1 + \cos(2\Delta\omega \cdot t)] \qquad (6)$$

$$I_{PD4} = A[1 - \cos(2\Delta\omega \cdot t)] \qquad (7)$$

where,

$$\Delta\omega = 4\pi \cdot \frac{\Delta x}{d} \qquad (8)$$

where Δx is the displacement of grating; d is the grating pitch.

3. Improved LDGI Design

To simplify the structure and improve the signal quality a new structure is proposed.

3.1 Optical path difference

The coherent length of semiconductor laser is limited to several millimeters only. Even in the coherent length the optical path difference should be eliminated to increase the fringe contrast. In the former structure the RHP plays the role to compensate the optical path difference. Therefore the RHP needs a nonstandard dimension. The manufacturing error and installation error of the RAP and RHP will influence the optical path difference.

3.2 Redundant beams

Too many optical surfaces will cause redundant reflection and refraction. The redundant beams may cause instable background light, which leads to the DC drift. Besides, if the diffraction beams are reflected to the grating again the higher-order diffraction will arise, which will lead to the disturbance with multiple frequencies.

Fig. 3(a) shows the distorted waveform with DC drift. Fig. 3(b) shows another distortion pattern with which the high peaks and low peaks appear alternately. With frequency-domain analysis a harmonic component of $1.5\,\Delta f$ is found, which means one of the diffraction beams are partially reflected to the grating again.
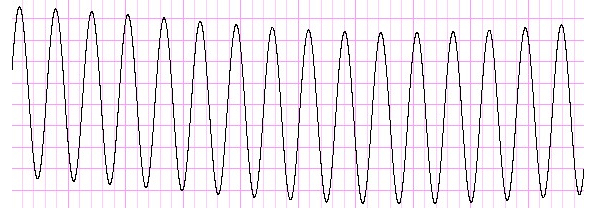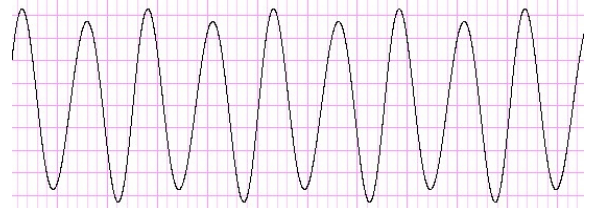

Fig. 3(a) Distorted waveform with DC drift

Fig. 3(b) Distorted waveform with harmonic disturbance

3.3 Improved optical system

To solve the above problems, an improved optical system is proposed, as shown in Fig. 4.
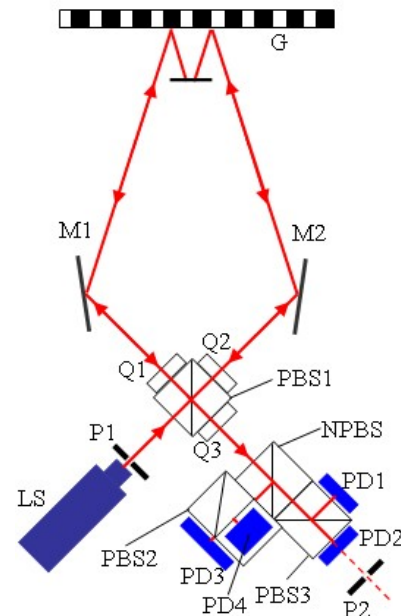
Fig.4 Improved design of LDGI (LS: laser diode, G: grating, PBSi: ith polarizing beam splitter, Mi: ith mirror, NPBS: non-polarizing beam splitter, Qi: ith quarter waveplate, PDi: ith photodetector. P: pinhole)

3.3.1 Elimination of optical path difference

In this new structure the left-arm and right-arm beams form a symmetrical structure, which will completely eliminate the optical path difference without any compensative optics.

3.3.2 Elimination of redundant reflection

The improved design uses fewer optical components, which will reduce the possibility of redundant reflection. The only possibility that may cause higher-order diffraction relies on the air gaps between PBS1 and the quarter waveplates. Because the PBS1, Q1, Q2 and Q3 have uniform thickness, the air gaps can be easily eliminated by tight pressing. They are carefully adhered together and glued. In this study some special fixtures are designed for adhering and gluing operations.

3.3.3 Other improved considerations

The proposed structure is also featured by some other improved designs.

The -1 diffraction beam of the right-arm beam and +1 diffraction beam of the left-arm beam cannot be ignored. In fact, they will cause background intensity by unpredictable reflection and refraction, which will add DC offsets onto the ideal signals. A black paper wall is inserted to block the unused laser beams.

The second improvement is to insert two pinholes. The pinhole P1 is used to limit the diameter of interference spot in order to eliminate a second smaller interference spot (called the ghost spot) in the sensitive area of the photodetector. The other pinhole P2 is installed in front of the photodetector PD2. Before the photodetectors are installed, P2 serves as the target mark. Only when the beam passes through P2 can it emit to the center of the photodetector,. Therefore, pinholes P1 and P2 can play the role of determining the best optical quality.

3.4 Assembly and adjustment

In this system there are two optical modules: PBS1, Q1, Q2 and Q3 form the interference generation module; NPBS, PBS2 and PBS3 form the phase shifting module. They are assembled respectively, with corresponding fixtures.

The laser diode together with pinhole P1 is fixed on the base plate firstly. Then the interference module is fixed, with the laser beam passing through the center of each optical component. The reflection mirror M1 is then installed to direct the laser beam to the grating at +1 diffraction angle and, by the diffraction law, reflects along the same path as the input beam. After that, the phase shift module is fixed and aligned to allow the laser beam passing through the pinhole P2. The photodetectors PD1-3 are, then, sequentially fixed to the corresponding PBS surfaces respectively. It is noted that at this stage, only one laser beam exits to P2. In that direction about 2m away, a target object is set to receive the laser spot. Then the reflection mirror M2 is installed and adjusted to make the spot exactly overlapped with the existing one on the target object. Besides, tiny movement of M2 is needed to get the best contrast. At last, the photodetector PD4 is fixed.

After the above processes of assembly, the system can be completely installed as a whole.

4. Signal Quality Evaluation

In order to describe the typical distortions shown in Fig. 3, two signal quality parameters, calibrated with 1mm travel length, are defined as:

$$Q_1 = \frac{\sigma_P + \sigma_V}{\overline{P} - \overline{V}} \times 100\%$$

$$= \frac{\sqrt{\frac{1}{n-1}\sum_{i-1}^{n}(P_i - \overline{P})^2} + \sqrt{\frac{1}{n-1}\sum_{i-1}^{n}(V_i - \overline{V})^2}}{\overline{P}_i - \overline{V}_i} \cdot 100\% \qquad (9)$$

$$Q_2 = \sum_{i=0}^{n} \frac{1 - \mathrm{sgn}[(P_i - P_{i-1})(P_{i+1} - P_i)]}{n} \times 100\%$$

$$= \sum_{i=0}^{n} \frac{1 - \mathrm{sgn}[(P_i - P_{i-1})(P_{i+1} - P_i)]}{n} \times 100\% \qquad (10)$$

where, P_i is the peak value of the ith wave cycle and V_i is the valley value of the ith wave cycle. Q_1 describes the distortion of the envelope curves. Q_2 describes the vibration frequency of the peak-to-peak values. For example, Fig. 3(a) shows a waveform with notable Q1 and negligible Q2, which means the background light is changing smoothly. Besides, the interference intensity variation will also increase the value of Q1. A big value of Q2, therefore, means a zigzag envelop curve which can hardly be processed. Fig. 3(b) shows a waveform with notable Q2, which means there is some harmonic disturbance, even though the interference intensity and the background light keep stable.

A pair of waveforms waveform of 1mm is sampled. With Eq. (9) and Eq. (10) the quality parameters are worked out: Q1=9%, Q2<1%. Compared with the former structure (Q1=12%, Q2=3.5%) the signal quality is obviously improved. Since the harmonic disturbance is negligible, with a software-based processor, the waveforms can be easily normalized, as shown in Fig. 5. With pulse counting and phase subdivision technique, the displacement can be calculated to nanometer resolution.
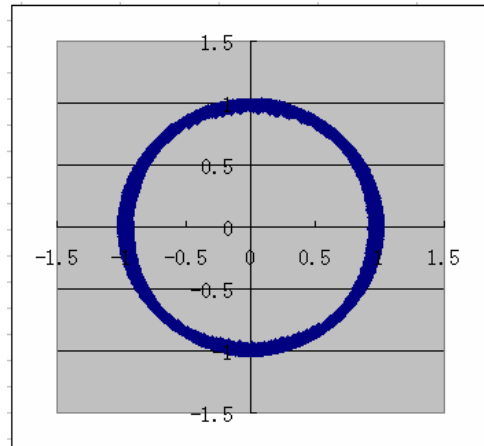

Fig. 5. Lissjous figure of the normalized waveforms

5. Positioning Experiments

To test the precision of the new sensor a positioning experimental system is configured as shown in Fig. 6. A laser interferometer HP5529A is used to calibrate this new LDGI sensor. The table is driven by an ultrasonic motor HR4 (Nanomotion Co.) on the opposite side.

A close-loop positioning controller with PID loop and neural network is employed [11]. The positioning experiment of each point is repeated five times. Table.1 shows the displacement measurement errors and the standard deviation.

The data show that in the travel length of 15mm, the standard deviation is within 10nm. Accumulated errors are clearly seen due to

the alignment error of the grating to the motion axis.

Some possible error sources were found as follows:

1. The quality of the holographic grating is important. The uniformity of the grating pitch and the reflection rate will influence the diffraction efficiency and accordingly alter the DC drift and amplitude.

2. Although the grating pitch is more stable than laser wavelength, the temperature is also an important error factor.

3. Electrical circuit noises, ground and surrounding facilities will cause measurement errors. When the table position is held by the close-loop controller, there's still reading variation within ±1nm.

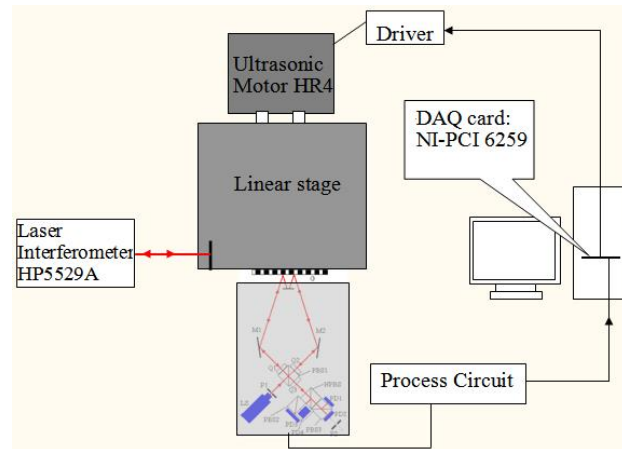Fig. 6 The experimental set-up for positioning test

Table.1 Experimental Data

Position(mm)	0.1	1	5	10	15
Error 1 (nm)	1	96	432	882	1315
Error 2 (nm)	2	105	421	881	1338
Error 3 (nm)	-1	88	439	861	1332
Error 4 (nm)	0	87	418	875	1321
Error 5 (nm)	3	99	425	876	1329
Average Error (nm)	1	95	427	877	1327
Standard Deviation (nm)	1.6	7.6	8.5	8.0	9.1

6. Conclusions

In this study a new grating-base interferometer is developed with the consideration of increasing the head-to-scale alignment tolerance. Compared with the former design, it shows some notable advantages: Fewer components are used to construct the optical system; A symmetrical structure is employed to eliminate the optical path difference; The best path is specified to eliminate the assembly uncertainty.

Positioning experiments show that the new sensor has the resolution higher than 1nm and the repeatability is within 10nm.

REFERENCE

1. Chen, X.H., Zhao, Y. and Li, D.C., "Review on Optical Nanometrology". Optical Technique.1999, 3, pp. 74-78.
2. Cramar, J.A., "Nanometer Resolution Metrology with the Molecular Measuring Machine". Meas. Sci. Technol. NO.16, pp. 2121-2128, 2005.
3. Chu, C.L. and Fan, K.C., "Design of a Digital Controller for Long-stroke Submicron Positioning stage", Proceedings of the 1st International Conference of Positioning Technology, Act-city, Hamamatsu, Japan, June 9-11, 2004, pp. 176-181.
4. Fan, K.C. and Su, C.D., "Error analysis for a diffraction grating interferometric stylus probing system". Meas. Sci. Technol. NO.12, pp. 482–490, 2001.
5. Fan, K.C. and Liu, Y.S., "A Linear Diffraction Grating Interferometer with High Accuracy", Proc. of SPIE Vol.6280, 628008, 2006
6. Fan, K.C., Fei, Y.T., Yu, X.F, Chen, Y.J., Wang, W.L., Cheng, F. and Liu, Y.S., "Development of a low cost Micro-CMM for 3D micro/nano measurements," Measurement Science & Technology, Vol. 17, pp. 524-532, 2006.
7. Fan, K.C. and Lai, Z.F., "A displacement spindle in a micro/nano level" Meas. Sci. Technol. NO.18, pp. 1710–1717, 2007.
8. Fan, K.C., Li, B.K. and Liu, C.H., "A diffraction grating scale for long range and nanometer resolution," Proc. of SPIE Vol. 7133, 71334J-1, 2009.
9. Birch, K.P., "Optical Fringe Subdivision with Nanometric Accuracy" Precision Engineering, Vol. 12 No. 4, pp. 195-198, 1990.
10. Wen, P., and Hsu, D.H., "Direct subdivision of Moire fringe with CCD," Proceedings of SPIE, Vol. 1230, pp. 165-166, 1990.
11. Fan, K.C. and Cheng, F., "Nanopositioning Control on a Commercial Linear Stage by Software Error Correction", Nanotechnology and Precision Engineering, Vol.4, No.1, pp. 1-9, 2006.